

## STOCHASTICITY, COMPLEX SPATIAL STRUCTURE, AND THE FEASIBILITY OF THE SHIFTING BALANCE THEORY

BRENDAN O'FALLON<sup>1,2</sup> AND FREDERICK R. ADLER<sup>1,3,4</sup>

<sup>1</sup>Department of Biology, University of Utah, Salt Lake City, Utah 84112

<sup>2</sup>E-mail: brendanofallon@fastmail.fm

<sup>3</sup>Department of Mathematics, University of Utah, Salt Lake City, Utah 84112

<sup>4</sup>E-mail: adler@math.utah.edu

**Abstract.**—Sewall Wright's shifting balance theory of evolution posits a mechanism by which a structured population may escape local fitness optima and find a global optimum. We examine a one-locus, two-allele model of underdominance in populations with differing spatial arrangements of demes, both analytically and with Monte Carlo simulations. We find that inclusion of variance in interpatch connectivities can significantly reduce the number of generations required for fixation of the more favorable allele relative to island and stepping-stone models. Although time to fixation increases with migration rate in all cases, the presence of one or two relatively isolated demes may reduce the number of generations by 80% or more. These results suggest that the shifting balance process may operate under less restrictive conditions than those found with a simple spatial arrangement of demes.

**Key words.**—Fitness landscape, Sewall Wright, shifting balance theory, spatial structure, underdominance.

Received July 19, 2005. Accepted January 5, 2006.

During the first part of the 20th century, Sewall Wright (1931) proposed an alternative mode of evolution. Influenced by his studies of interaction systems of genes (Provine 1971), Wright became concerned that selection on simple additive traits may not provide a complete story of adaptive evolution. In particular, if interactions among genes are strong and relatively common, a certain combination of alleles may provide intermediate fitness, a very different combination of alleles may endow higher fitness, and blends of these two alternative genotypes may be less fit than either one alone. This led to Wright's lasting metaphor of an adaptive landscape, where multiple peaks of relatively high fitness, each representing a particular combination of alleles, are separated by valleys of low fitness. Because Fisherian selection (Fisher 1930) may only increase the mean fitness of a population, it alone cannot account for transitions between isolated adaptive peaks separated by valleys of reduced fitness.

To explain these hypothetical transitions Wright (1931) proposed his famous and controversial shifting balance theory (SBT), a mechanism by which a given population may explore a rugged adaptive landscape. The shifting balance may only operate in a metapopulation and occurs in three phases. In phase I, a single subpopulation, or deme, wanders across an adaptive valley by drift alone, toward the domain of attraction of a higher peak. In phase II, natural selection drives the deme up to the higher peak, that is, the deme becomes fixed for the more fit combination of alleles. In phase III, the deme now fixed at the higher peak exports individuals to the rest of the population and thus incites a global shift to the fitter peak. Although Wright imagined that demes with higher fitness would export more individuals, this is not required for the SBT.

Whether or not the SBT operates in nature has remained a subject of debate since the theory was proposed. Many authors have modeled various aspects of the process (Barton and Rouhani 1991, 1993; Crow et al. 1990; Phillips 1993; Gavrillets 1996; Coyne et al. 1997; Peck et al. 1998), often arriving at different conclusions regarding its theoretical

plausibility. Wade and Goodnight (1991) found that the process may operate in *Tribolium castaneum* under laboratory conditions and a specific experimental structure (but for a different interpretation of these results see Coyne et al. 1997), and Blum (2002) found some evidence for phase III in a movement of a *Heliconius* hybrid zone. To date, there have been no uncontested observations of the shifting balance (SB) process in nature.

Coyne et al. (1997) published a thorough critique that assessed the SBT from both theoretical and empirical perspectives. They concluded "We have found no compelling evidence that Wright's SBT accounts for the evolution of a single adaptation, much less a significant proportion of adaptations, in nature" (1997, p. 665). Regarding the theoretical aspects, they admitted, "Theory shows that the SB can sometimes be an efficient mechanism of selection, but only under restrictive conditions" (p. 664).

Several authors responded with more favorable views of the SBT. Wade and Goodnight (1998, 2000) defended Wright's view from both empirical and theoretical perspectives (for a response see Coyne et al. 2000). Peck et al. (1998, 2000) argued that models that include local interactions among demes and stochastic migration facilitate the SBT. Their simulation model included stochastic migration among 49 demes arranged in a  $7 \times 7$  lattice. For some parameter combinations phase III of the SBT proceeded, whereas in deterministic models it did not. Unfortunately, the analysis suffered from the low numbers of simulation replicates (only seven trials for each parameter combination) and restricted time scale examined (a maximum of 30,000 rounds for all trials).

In previous analyses of the SBT, many authors have assumed a relatively simple spatial arrangement of demes. Some authors have restricted their analysis to only two demes (Crow et al. 1990; Phillips 1993; Peck et al. 2000), with one deme initially fixed for the more fit combination of alleles. Because the frequency of the more fit allele combination begins at 50%, these models probably do not correspond to

TABLE 1. Parameters and values used in the simulation and mathematical model.

Symbol	Values	Description
$s$	0.01, 0.05, 0.1	relative advantage of AA and disadvantage of Aa
$N$	50, 100, 200	number of individuals per deme
$m_{ij}$	many (0.0–0.05)	per individual probability of migration from deme $j$ to deme $i$
$m$	0.000–0.035	mean global migration rate
$D$	10, 20, 40	number of demes
$\mu$	0.0001	two-way mutation rate
$d_e, d_i$	0, 1, 2, 4	effect of isolation of demes on export and import (in nonuniform export MDK model)
$k$	0, 2, 3, 6	number of isolated demes (in MDK model)
$\gamma$	0, 1, 5	strength of interdeme selection, relative to individual selection

SB as it may exist in the natural world (see Gavrillets 1996). In other cases either an island (Lande 1985; Barton and Rouhani 1993) or a one- or two-dimensional stepping-stone (Barton and Rouhani 1991; Gavrillets 1996) model was used. Under these assumptions and others regarding the strength of selection and probability of migration, analytic formulas for the distribution of demic states, probabilities of fixation, and times to fixation can sometimes be achieved (Lande 1979, 1985; Barton and Rouhani 1993). Several authors have noted that fixation of underdominant mutations is more likely if the initially fixed deme is at the edge of the world of demes (Boorman and Levitt 1980; Gavrillets 1996) or in a region of low neighborhood size (Barton and Rouhani 1991), but no studies have explicitly examined the impact of spatial complexity on the feasibility of the SBT.

In this paper we develop and analyze a model that relaxes the assumptions of simple population structure and determinism. Our goals are twofold. First, we build upon Peck et al.'s (1998) results and present a thorough investigation of the SBT in a purely stochastic world. Second, we relax the assumption of simple population structure, defined as zero variance in interdeme connectivity, and compare the efficiency of island and stepping-stone models to both random and clumped distributions of demes. We present simulations and a mathematical approximation. The model is general enough, in principle, to incorporate any distribution of interpatch connectivities, as well as all three phases of the process.

## METHODS

We examine a one-locus, two-allele model with heterozygote disadvantage. The fitness of an *aa* individual is one, the fitness of the heterozygote is  $1 - s$ , and the fitness of the AA homozygote is  $1 + s$  (see Table 1 for a list of parameters used).

### The Simulation

The simulation takes place in discrete generations, with each generation involving three independent events; mutation, reproduction, and migration. The number of individuals of each genotype in each deme is an explicit variable in this individual-based model. Mutation takes place each round, with each allele mutating to the other type with probability  $\mu$ .

Prior to selection, individuals are assumed to mate randomly and produce a large number of zygotes in Hardy-Weinberg proportions. To determine the composition of the

population in the next generation, zygotes are sampled with probabilities determined by genotypic fitnesses; for example, the probability of selecting an AA individual is  $p^2(1 + s)/W(p)$ , where  $p$  is the frequency of the A allele and  $W(p)$  is the mean fitness of the population. Zygotes are sampled until the population contains exactly  $N$  individuals.

Migration takes place after mutation and selection in every generation. Given a patch connectivity  $m_{ij}$ , a group of migrants was created that contained a Poisson distributed number of individuals with mean  $Nm_{ij}$ . Individuals were randomly removed from the source deme, independent of genotype. The individuals in the migrant group were then placed in the destination deme.

### The Migration Model

Our goal was to render migration in a manner more similar to nature than island or stepping-stone models. Given an arbitrary distribution of demes on the unit torus, a matrix of connectivities between all demes was constructed such that the connectedness of demes  $i$  and  $j$  was given by  $c_{ij} = (d_{ij}^2 + 0.01)^{-1}$ , where  $d_{ij}$  is the distance separating the demes. We assumed a fixed global per capita migration probability,  $m$ , such that each individual has probability  $m$  of migrating in a given generation, irrespective of the distances to nearby demes. To accomplish this, the rows of the matrix of deme connectivities were divided by their average, divided again by the number of demes in the metapopulation, and then multiplied by  $m$ . Thus, the sum of each row in the matrix was  $m$  (ignoring the diagonal entries). The sums of the columns of the matrix, which represent the likelihood of a deme to receive immigrants, were left to vary. Because the size of each deme was held constant at  $N$ , each deme exports on average  $Nm$  individuals per round, but demes vary in how many individuals they receive each round.

### Generating Patchy Distributions of Demes

In addition to assessing the effect of spatial distributions where the location of each deme was selected independently (random distributions), we also sought to examine clumpy patterns, where the variance in deme connectivity was increased. Clumpy patterns were generated following Adler and Nuernberger (1994). We first define a clumpiness index,  $G_i$ , for each deme  $i$  such that

$$G_i = \frac{1}{D-1} \sum_{j \neq i} \frac{1}{0.01 + d_{ij}^2}. \quad (1)$$

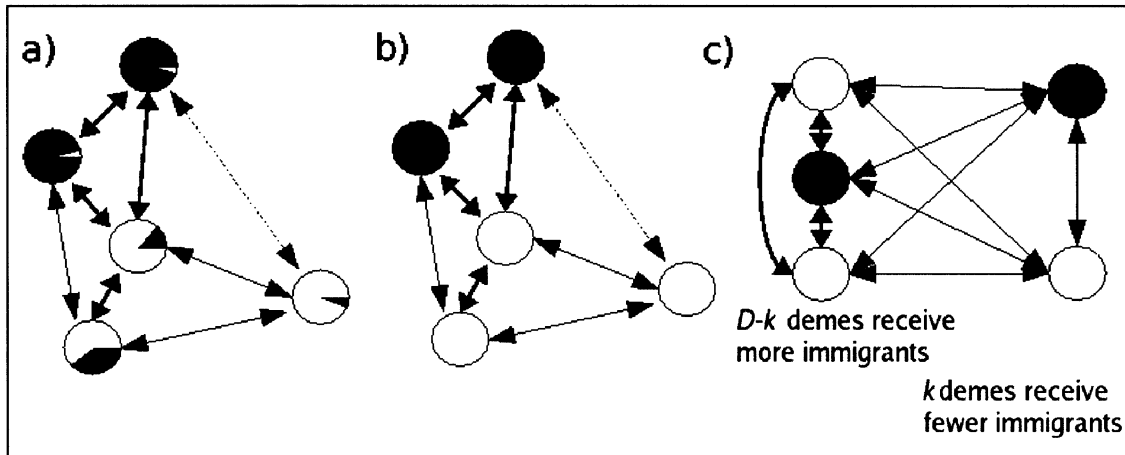


FIG. 1. (a) In the simulation, each deme has a large number of possible states (proportions of the  $A$  allele, represented by black area), and every location is unique. To simplify calculations, we make two assumptions: (b) every deme is always fixed for one or the other allele, and (c) only two locations exist, clumped and isolated. Migration probability between two demes is indicated by the weight of the line connecting them.

During each iteration of the algorithm, a new potential location is selected on the torus for every deme. The probability of moving a deme to this new location is an increasing linear function of the  $G$ -value at the new point. The procedure is repeated until patterns of desired clumpiness are obtained. Patterns can be described by the mean  $G$  over all demes. Random patterns produced an average  $G$  of near 11. Patterns that match our intuitive notion of clumpy generally have a  $G$ -value greater than 20. In addition to random patterns, we examined patterns that had an average  $G$  of 20 or 25.  $G$  was positively correlated with variance among column sums of the matrix of deme connectivities in the range of indices considered (correlation coefficient  $\approx 0.73$ ). Demes were not moved during any simulation replicate, but new patterns were generated for each replicate for the random and clumped patterns.

#### A Markov Chain Approximation

Because our simulation has a finite number of states and probabilities of transitions between these states are, in principle, calculable, a single Markov chain can describe the entire system. However, the number of states is too large  $(2N + 1)^{D+1}$  to analyze, and thus we make two assumptions to simplify the calculations. First, we assume the demes spend their time fixed for one or the other allele. This reduces the number of states for a single deme from  $2N + 1$  to 2. Second, we allow only two possible connectivities of demes, clumped and isolated. This assumption allows us to examine the effects of variance in deme connectivity, but not the importance of local effects because demes in each location class are identical. Because all demes in a given location receive the same number of immigrants (on average), the number of possible states for the entire metapopulation is greatly reduced (see Fig. 1).

We first calculate the probability that a single deme with  $j$   $A$  alleles (and  $2N - j$   $a$  alleles) will have  $i$   $A$  alleles after one generation. Each generation consists of one round of of mutation, selection, and given immigration rates of  $m_A$   $A$

alleles and  $m_a$   $a$  alleles. Using this information, we can calculate the probability that a deme fixed for  $a$  crosses the adaptive valley after a certain number of generations, and likewise for the transition from  $a$  to  $A$ . Because these probabilities depend on the number of  $A$  and  $a$  alleles entering the deme (denoted by  $m_A$  and  $m_a$ , respectively), we express them as functions:  $P(m_A, m_a)$  for the transition from fixed for  $a$  to fixed for  $A$  and  $Q(m_A, m_a)$  for the reverse transition.

Second, we compute  $m_A$  and  $m_a$  for a given distribution of demes and deme states, and using  $P(m_A, m_a)$  and  $Q(m_A, m_a)$  we calculate the probability that a metapopulation with  $j$  demes fixed for  $A$  will switch to having  $i$  demes fixed for  $A$ . We do this first for an island model and then extend our analysis to a metapopulation with two types of demes, isolated and clumped.

#### Modeling dynamics within demes

The mathematical model begins with a description of the dynamics within a particular deme. Because the number of possible allelic states is not too large and the simulations take place in discrete rounds, a Markov chain approach may be used to obtain a probability distribution for the state of a given deme at any time. Let the states of the system be the number of  $A$  alleles present; there are then  $2N + 1$  possible states. The probability that a deme in state  $j$  in one round will be in state  $i$  the next round,  $T_{ij}$ , is a combination of three independent factors, mutation, migration, and selection. Thus, the matrix of transition probabilities may be decomposed into three matrices, one for each factor.

Let  $U$  be the matrix describing transition probabilities due to mutation alone. Each element,  $U_{ij}$ , may be expressed as the following:

$$U_{ij} = \sum_{k=0}^{2N} B(j - i + k, j, \mu) B(k, 2N - j, \mu), \quad (2)$$

where  $B$  is the binomial probability density function



$$B(m, n, p) = \binom{n}{m} p^m (1 - p)^{n-m}. \quad (3)$$

The first function in the sum represents the probability that  $j - i + k$  of the  $j$   $A$  alleles present will mutate to  $a$ , the last function the probability that  $k$  of the  $2N - j$   $a$  alleles will mutate to  $A$ . In the actual calculations, we ignored the possibility that mutation changed the number of  $A$  alleles in a deme by more than 10 in any given generation.

The matrix of transition probabilities due to selection,  $\mathbf{S}$ , is

$$S_{ij} = \binom{2N}{i} \left[ \frac{pW_A(p)}{W(p)} \right]^i \left[ 1 - \frac{pW_A(p)}{W(p)} \right]^{2N-i}, \quad (4)$$

where  $p = j/2N$ .

Finally, for a known probability of arrival of  $A$  alleles and  $a$  alleles, the matrix that describes transitions due to immigration,  $\mathbf{R}$ , can be found by noting that the number of  $A$  alleles that are replaced by an arrival of  $k$  individuals is a hypergeometric random variable with parameters  $2N$ ,  $j$ , and  $k$ . Because arrivals of both types of alleles are approximately Poisson distributed (we use the Poisson approximation of the binomial; Adler 2005), each element in the matrix is the sum of a number of alternative probabilities:

$$\begin{aligned} \mathbf{R}_{ij} = & \sum_{k=0}^{\infty} \sum_{l=0}^{\infty} H(2N, k + l, j, j - i + k) \\ & \times M_{AA}(k, m_{AA}) M_{aa}(l, m_{aa}), \end{aligned} \quad (5)$$

where  $k$  and  $l$  index the number of arriving  $A$  and  $a$  alleles,  $H$  is the hypergeometric density function,  $M_{AA}(k, m_{AA})$  represents the probability of receiving  $k$   $A$  alleles given a Poisson-distributed flow of  $AA$  individuals with mean  $m_{AA}$ , and similarly for  $M_{aa}(l, m_{aa})$ . Given these three matrices, their product  $\mathbf{T} = \mathbf{RSU}$  gives the matrix of transition probabilities for allelic states within a single deme.  $\mathbf{T}$  may then be used to calculate the probability of transition from the fixed for  $A$  state to any other state, and the reverse, given a known immigration rate of  $A$  and  $a$  alleles.

#### Modeling dynamics between demes

To apply the within-deme processes to the entire metapopulation, we assume that demes are always either fixed for  $A$  or  $a$ . We call these states shifted and unshifted, or simply on or off, respectively. Although this assumption appears to contradict our earlier description of within-deme dynamics, an explicit within-deme process is still necessary to compute the  $P$  and  $Q$  functions described above. Thus, we assume that selection is strong enough that few demes have intermediate fitness, which is consistent with Wright's idea of an adaptive valley that is difficult to cross by drift alone. We begin by considering the probability that a patch fixed for the  $a$  allele and receiving a Poisson-distributed flow of  $m_A$   $AA$  individuals and  $m_a$   $aa$  individuals per generation crosses the valley in a certain number of rounds, say  $r$ . This may be found by multiplying a vector with all probability in the 0 state by  $\mathbf{T}(m_A, m_a)^r$ , and then taking the sum of  $v$  elements at the end of the vector that correspond to fixation for the  $A$  allele, where  $v$  depends on  $s$  in general, but was taken to be 100 for the results shown here. Repeating this process for a wide range of  $m_A$  and  $m_a$  combinations produces a matrix of probabilities

of transitions to the shifted state. Interpolating the values in this matrix yields a function that describes the probability of transition to the shifted state given a certain flow of  $A$  and  $a$  alleles, for a particular number of generations, which we call  $P(m_A, m_a)$ . Put simply,  $P(m_A, m_a)$  describes the probability that a deme fixed for  $a$  and receiving a certain flow of  $AA$  and  $aa$  individuals becomes fixed for  $A$  in  $r$  generations. Similarly, the function  $Q(m_A, m_a)$  describes the probability of transition from the shifted to the unshifted state. For this analysis we chose  $r = 100$  generations, approximately the time to fixation of an  $A$  allele, conditional on fixation.

Given the functions  $P(m_A, m_a)$  and  $Q(m_A, m_a)$ , it is possible to calculate the probability of changes of state for the entire metapopulation. We begin here with the island arrangement and then expand our method to a pseudospacial model that approximates the more complex spatial structure used in the simulations.

For an island arrangement of demes, using our assumption that demes are always fixed for either one or the other allele, the entire metapopulation has only  $D + 1$  states, where  $D$  is the number of demes. If there are  $j$  demes fixed for  $A$ , and each of these exports  $m$   $A$  alleles each round, then all demes experience a Poisson-distributed flow of  $jm$   $AA$  individuals and  $(D - j)m$   $aa$  individuals (from the remaining, unshifted demes) each generation. The probability of an unshifted deme becoming shifted is then  $P(jm, (D - j)m)$ , and the probability of a shifted deme becoming unshifted is  $Q(jm, (D - j)m)$ . Thus the total number of demes that switch from unshifted to shifted is a binomial random variable with parameters  $D - j$  and  $P(jm, (D - j)m)$  and the number of off demes that switch to on is also binomially distributed but with parameters  $j$  and  $Q(jm, (D - j)m)$ . Implicit in this framework is the assumption that demes shift only once during the  $r$  generations. This assumption is accurate for phases I and II of the process, because shifts are infrequent during this period, but potentially inaccurate during the midst of phase III. Nonetheless, the approximation appears robust (see Comparison of Simulation and Mathematical Results, below).

To compute the probability that a world with  $j$  demes on becomes a world with  $i$  demes on, we must sum over a number of different possibilities that represent different paths from  $j$  to  $i$ . For instance, if  $j$  is 3 and  $i$  is 5, we must include the probability that two additional demes turned on and zero turned off, as well as the probabilities that three demes turned on and one turned off and that four turned on and two turned off, and so on.

Putting all this together yields an expression for  $\mathbf{V}_{ij}$ :

$$\begin{aligned} \mathbf{V}_{ij} = & \sum_{k=0}^D \binom{D-j}{k} P^k (1 - P)^{D-j-k} \\ & \times \binom{j}{k-i+j} Q^{k-i+j} (1 - Q)^{i-k}. \end{aligned} \quad (6)$$

where the arguments to the  $P$  and  $Q$  functions are  $(jm, (D - j)m)$ .

#### A Pseudospacial Model

In principle, the above method could be applied to metapopulations of arbitrary spatial structure and number of

demes. However, even with the two state approximation, the number of possible states is  $2^{D+1}$  if every deme is unique. To further reduce the number of possible states, we constructed a model that captures some of the elements of complex spatial structure, namely variance in immigration potential among demes, but that uses only two types of demes. In this construction, we imagine  $k$  of the  $D$  demes are isolated by a factor of  $d$ , such that immigration to these demes, given a particular  $m$ , is reduced to  $m(1 - d/k)$ . To ensure that the global average migration rate remains equal to  $m$ , the remaining  $D - k$  demes experience increased migration of  $m(1 + d/(D - k))$ . The parameter  $d$  describes the degree of isolation of the  $k$  demes and ranges between zero (no isolation of demes, which reduces to the island model) and  $k$  (demes are so isolated they receive no immigrants). We refer to this as the MDK model; often we write MDK( $d, k$ ) to indicate precise values of  $d$  and  $k$  used for a given calculation. It is important to note that varying  $d$  does not affect the mean migration rate in the metapopulation, it increases only the variance in deme connectivity.

To facilitate comparison to the spatial models, it would be convenient to calculate a  $G$ -value for an arbitrary MDK model. Unfortunately, an unambiguous  $G$  cannot be calculated given an arbitrary matrix of connectivities because information about the absolute distances is lost when distances are converted to connectivities. The most accurate comparison between the MDK and spatial models is the coefficient of variation among column sums of the connectivity matrix, which is a more direct measure of variation in migration probabilities.

The MDK model has  $(k + 1)(D - k + 1)$  possible states, and each state represents a unique number of shifted, isolated demes and shifted, nonisolated demes. The calculations for the transition matrix are similar to those for the island model, but both types of demes must be treated separately. For simplicity, we refer to  $k$  demes that receive fewer migrants as the isolated demes and the remainder as the clumped demes.

For a given state index, let  $j_i$  indicate the number of isolated demes on and  $j_c$  indicate the number of clumped demes on. The number of isolated demes that switch from on to off in a given number of generations is assumed to be independent of the number of clumped demes that switch. Because all isolated demes are identical in terms of the expected number of migrants they receive and all demes are identical in terms of the migrants they export, a simple expression may be written for the probability of transitions between states of isolated demes alone. By definition, all isolated demes receive, on average,  $m(1 - d/k)$  individuals per round. Given  $j_c + j_i$  shifted demes in a given generation (and  $D - j_c - j_i$  unshifted demes), every isolated deme experiences a mean flow of

$$m_{iA} = (j_c + j_i)m\left(1 - \frac{d}{k}\right)$$

AA individuals per round and

$$m_{iA} = (D - j_c - j_i)m\left(1 - \frac{d}{k}\right)$$

aa individuals per round. Thus, every isolated deme that is

off has independent probability  $P(m_{iA}, m_{i,a})$  of turning on. Similarly, every isolated deme that is on has an independent probability  $Q(m_{iA}, m_{i,a})$  of turning off.

As with the island model, the total number of isolated shifted demes that unshift and isolated unshifted demes that shift is the the sum of two binomial random variables with parameters  $P(m_{iA}, m_{i,a})$  and  $Q(m_{iA}, m_{i,a})$ . To find the probability of transition to a particular number of isolated shifted demes,  $i_i$ , we sum over all probabilities of transitions that lead to  $i_i$  isolated shifted demes from  $j_i$  isolated shifted demes. The total probability that a world with  $j_i$  isolated shifted demes and  $j_c$  clumped shifted demes transitions to a world with  $i_i$  isolated shifted demes is given by:

$$\begin{aligned} \Delta_i = & \sum_{l=0}^k \binom{k - j_c}{l} P(m_{iA}, m_{i,a})^l \\ & \times [1 - P(m_{iA}, m_{i,a})]^{k-j_c-l} \\ & \times \binom{j_i}{l - j_i - i} Q(m_{iA}, m_{i,a})^{l-j_i-i} \\ & \times [1 - Q(m_{iA}, m_{i,a})]^{i-l}. \end{aligned} \quad (7)$$

where the arguments to  $P$  and  $Q$  are  $(m_{iA}, m_{i,a})$ .

Similar reasoning follows for the probability of transition to a given number clumped demes. In this case  $m_{cA}$  and  $m_{c,a}$  are given by

$$\begin{aligned} m_{cA} &= (j_c + j_i)m\left(1 + \frac{d}{D - k}\right) \quad \text{and} \\ m_{c,a} &= (D - j_c - j_i)m\left(1 + \frac{d}{D - k}\right), \end{aligned}$$

respectively. Multiplying the probabilities for the transitions between numbers of isolated shifted demes and numbers of clumped shifted demes, and taking care to index properly, yields a matrix with  $(k + 1)(D - k + 1)$  rows and columns that describes the probability of stochastic shifts between all possible states of the metapopulation.

Once this matrix has been calculated, a straightforward procedure leads to calculation of the expected first passage time (FPT; Bhat and Miller 2002), the expected number of rounds until the process, initially in state  $i$ , reaches state  $j$  for the first time. We are particularly interested in the expected number of rounds for the process to proceed from a state with zero shifted demes to a state with  $D$  shifted demes. This was taken to be a combined measure of the efficiency of all three phases of the SBT.

#### Identification of Steady States

A deterministic approximation of this process may be obtained by considering  $x$ , the fraction of demes that are shifted at a given time. If the total number of demes is large, we may ignore stochastic fluctuations in the numbers of shifted demes and focus, for the moment, on identifying equilibria. The change in  $x$  after one  $r$ -round time step may be found by using the functions  $P(m_A, m_a)$  and  $Q(m_A, m_a)$ . In an island model, all demes export and receive the same number of migrants,  $m$ . If  $x$  is the fraction of shifted demes, all demes receive  $xm$  AA individuals (as a fraction of total deme size)

and  $(1 - x)m$  *aa* individuals. After one time step, the fraction of shifted demes is the sum of those shifted demes that did not unshift and the unshifted demes that did shift:

$$x' = x\{1 - Q(xm, (1 - x)m)\} + (1 - x)P(xm, (1 - x)m). \quad (8)$$

Equilibria occur where  $x' = x$ , and are obtained by setting  $x_{eq} = x' = x$  and solving for  $x_{eq}$ . Doing so yields:

$$x_{eq} = \frac{P(xm, (1 - x)m)}{P(xm, (1 - x)m) + Q(xm, (1 - x)m)}. \quad (9)$$

Similar calculations can be carried out for the MDK model, but the system will have two state variables, one for isolated demes and another for clumped demes. Import to isolated demes is decreased by a factor of  $(1 - d/k)$ , and import to clumped demes is increased by a factor of  $[1 + d/(D - k)]$ .

Treating  $m$  as a bifurcation parameter, we can assess the number, location, and stability of equilibria for different levels of migration. This procedure is a discrete-time analogue of similar calculations carried out by Barton and Rouhani (1993), who used Wright's formula and simplifications thereof to approximate the distribution of demic states. We further simplify and assume that demic states are Bernoulli random variables, with probabilities of transition given by  $P$  and  $Q$  and the state of the migrant pool. Our method also takes into account the history of a deme in question, because migration events several generations ago affect  $P$  and  $Q$ , and thus may alter the probability of a shift. This approach is nearly identical to Hanski's incidence function model of patch occupancy in spatially realistic metapopulations (Hanski 1994), with  $P$  and  $Q$  describing the colonization and extinction probabilities of the *A* allele.

In a diffusion analysis the two quantities of interest are  $M$ , the expected change in gene frequency as a function of the current frequency, and  $V$ , the variance of that change (Ewens 1979). Modifying equation (8) by subtracting the current allele frequency  $x$  yields an expected change as a function of the present state. The variance in this quantity is given by the sum of two binomial random variables, the number of demes switching from fixed for *A* to fixed for *a*, and vice versa. The two random quantities are independent by assumption. For the island model, the variance is given by:

$$V = \frac{P(1 - P)}{D - k} + \frac{Q(1 - Q)}{k}, \quad (10)$$

where we have omitted the dependence on  $x$  and  $m$  for clarity. Although  $M$  and  $V$  in principle may be used to calculate, for example, a global probability of fixation, the complicated form of  $P$  and  $Q$  prohibit a simple expression for this and other quantities of interest. If simple expressions for  $P$  and  $Q$  can be found, then the methods of diffusion analysis may allow for an analytic approximation of times to and probabilities of fixation, as well as an expression for the critical migration rate.

#### Alternative Migration Models

Our previous assumption of uniform export from all demes may in some cases be unrealistic. Here we relax this previous

assumption and examine models that include isolation by distance for both import and export. We can also investigate the importance of Wright's original idea that SB is driven by greater export from demes with higher mean fitness.

To include differential export, we assume that export is decreased by distance in exactly the same fashion as import. In the MDK model, this means that isolated demes export  $Nm(1 - d/k)$  individuals on average and clumped demes export  $Nm(1 + d/(D - k))$  individuals, hence average export remains constant at  $Nm$  for any choice of  $d$  or  $k$ . Because distance may have different effects on the export and import of individuals from the demes, we separate the degree of isolation of export from import by writing  $d_e$  and  $d_i$ , respectively. Given this description, the average flow of individuals from an isolated deme to another isolated deme is  $Nm(1 - d_i/k)(1 - d_e/k)$ , and the flow from clumped demes to isolated demes is  $Nm(1 - d_i/k)[1 + d_e/(D - k)]$ . Flow into clumped demes follows similarly. The case  $d_e = 0$  reduces to the uniform export case where distance has no effect on export, and  $d_e = d_i$  means distance has similar effects on import and export. We are particularly interested in the case where individuals have some innate tendency to leave a deme, but the destination is influenced only by distance to that deme, which implies  $d_e < d_i$ .

We also examined the impact of differential export from demes of higher mean fitness. We begin by introducing a new parameter,  $\gamma$ , which describes the degree to which the mean fitness of a deme affects its export, and thus can be thought of as the parameter that translates the individual selection coefficient,  $s$ , to the group selection coefficient. Export from the deme is given by  $m[1 + \gamma(W - 1)]$ , where  $W$  is the mean fitness of the deme.  $\gamma = 0$  reduces to the basic model of uniform export described above,  $\gamma = 1$  implies that export is altered by a factor of  $W$ , so a deme fixed for *a* exports on average  $Nm$  individuals, but a deme fixed for *A* exports  $Nm(1 + s)$  on average.

## RESULTS

### Identification of Equilibria

The number and location of equilibria of the deterministic approximation (9) are presented in Figure 2. With  $m$  less than about 0.0125, the metapopulation progresses to the single stable equilibrium at the top of the figure, which corresponds to global fixation for *A*, regardless of population structure. However, as  $m$  increases above 0.0125 in the island model (Fig. 2a), the system undergoes a saddle-node bifurcation and a new pair of equilibria appears. The new stable equilibrium corresponds to a state with nearly zero shifted demes for all levels of  $m$ . The distance between the new stable and unstable manifolds corresponds to the level of difficulty of stochastic transitions between the two stable equilibria and increases with  $m$ . These results are qualitatively similar to those presented by Barton and Rouhani (1991, 1993), who also found deterministic progression of the SBT for low  $m$  and two stable equilibria for higher  $m$ .

For the MDK model there are two sets of equilibria, one for the isolated demes and another for the clumped demes (Figures 2b, 2c). As isolation of the  $k$  demes increases the bifurcation point associated with these demes moves right,



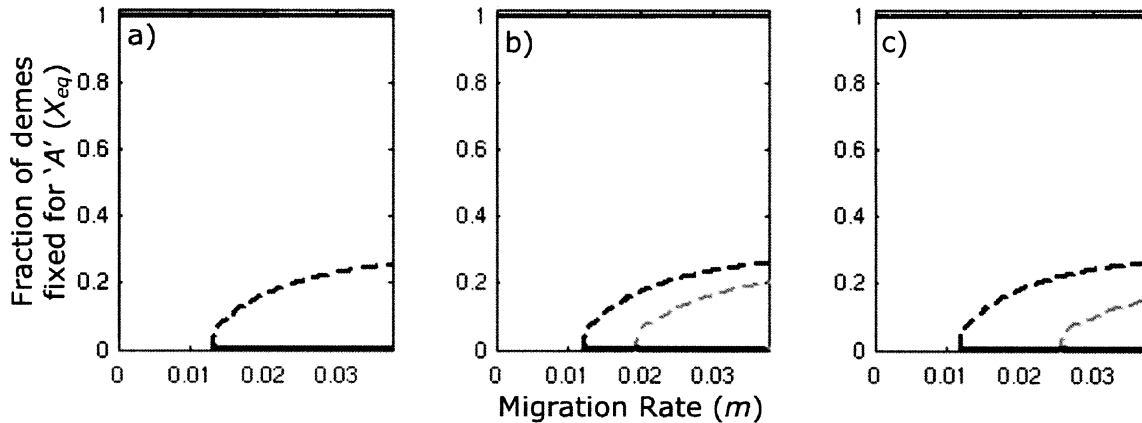


FIG. 2. Bifurcation diagram of equilibria of (a) an island, (b) MDK(1, 3), and (c) MDK(1.5, 3) (see text for explanation). Black lines correspond to equilibria for the high-import demes, gray lines are equilibria for the low-import demes. A stable equilibrium always exists at  $x \equiv 1$ , which corresponds to near global fixation for the beneficial allele  $A$ . As  $m$  increases, the system undergoes a saddle-node bifurcation and new equilibria appear; a stable manifold that corresponds to near global fixation for the  $a$  allele and an unstable manifold that separates the two stable states.

indicating that the isolated demes move to the fixed for  $A$  state deterministically for a greater range of migration rates. The manifold for the clumped demes is relatively unaffected by the presence of isolated demes. For intermediate  $m$ , two outcomes are possible: the population may remain polymorphic with the isolated demes fixed for  $A$  while the clumped demes remain at  $a$ , or the presence of the isolated fixed demes may drag the clumped demes across the barrier and to the upper manifold.

#### Simulation Results for Differing Spatial Structures

To examine the effect of the spatial arrangement of demes, we compared the FPT observed for the island model at a variety of migration rates to the FPT observed for random, clumped, and the MDK pseudospacial model used in the mathematical analysis. The MDK model examined had three isolated demes, and each deme was isolated by a factor of  $2/3$  ( $k = 3$ ,  $d = 2$ ), so that they received about one-third of the immigration of the clumped demes. The mean FPT of 50 simulation replicates for all spatial arrangements is plotted in Figure 3. A new pattern was generated for every replicate of every simulation where appropriate, and each replicate was run for a maximum of  $10^7$  generations. We show here the results for  $s = 0.05$ , but qualitatively similar results occur for  $s = 0.01$  and  $s = 0.1$  (results not shown). At higher migration rates for some spatial patterns (island and two-dimensional stepping-stone), the FPT was so great that few or no replicates reached global fixation before the maximum number of generations; this is indicated by a dotted line leading to the top of the figure.

Figure 3 demonstrates that, for relatively low migration rate (below 0.0125), the spatial arrangement of demes has little effect. Relatively infrequent migration ( $m = 0.001$ ) decreases FPT substantially when compared to the  $m = 0$  case, and FPT increases uniformly as  $m$  increases beyond 0.005. All replicates of all patterns proceed through the three phases, reaching global fixation for the  $A$  allele in several thousand generations. This is consistent with the result from the deterministic analysis where, for low  $m$ , the process proceeds

to the single stable state with all demes fixed for  $A$ . The value of  $m$  that yields that smallest FPT, and hence at which the entire shifting balance process operates most efficiently, is found at an intermediate value of 0.005 ( $Nm = 0.5$ ).

At higher migration rates, spatial structure has a profound effect. A random arrangement of demes, where this effect is slightest, has a mean FPT of 356,000 generations at a migration rate of  $m = 0.015$ , while the island model has a mean of greater than  $10^7$  generations. The two-dimensional stepping-stone model yields similar results to the random arrangement. Structures that incorporate more variance in deme connectivity (MDK and clumped) increase this effect, extending the range of migration rates at which the shifting balance proceeds by a factor of two or three.

The MDK(2,3) pattern appeared to be intermediate when compared with the two clumpy patterns; for most migration rates it yielded a mean FPT greater than clumped 25 and less than clumped 20. Interestingly, if the coefficient of variation in column sums of the migration matrix is taken to be a measure of the clumpiness of the migration probabilities, then the MDK(2,3) model appears slightly less clumpy than do the other clumpy patterns (CV for clumped 20  $\approx 0.325$ , MDK[2,3]  $\approx 0.30$ , random  $\approx 0.21$ ), and the intermediate result may be an artifact of sampling error. Nonetheless, this finding suggests that this relatively simple, pseudospacial pattern captures the important effects of complex spatial structure, and in later analyses we take the MDK pattern to be a surrogate for more realistic structure.

#### Comparison of Simulation and Mathematical Results

The calculated FPT and simulated FPT (with sample standard deviation) for the island and MDK models, for a variety of number of demes ( $D = 10, 20, 40$ , holding the total number of individuals,  $ND$ , constant at 2000), are compared in Figures 4a–c. The mathematical approximation works well for a range of migration rates, although it yields too high an estimate for the  $m = 0$  case and becomes more accurate as the number of demes increases and the number of individuals per deme decreases. This last is an expected consequence of

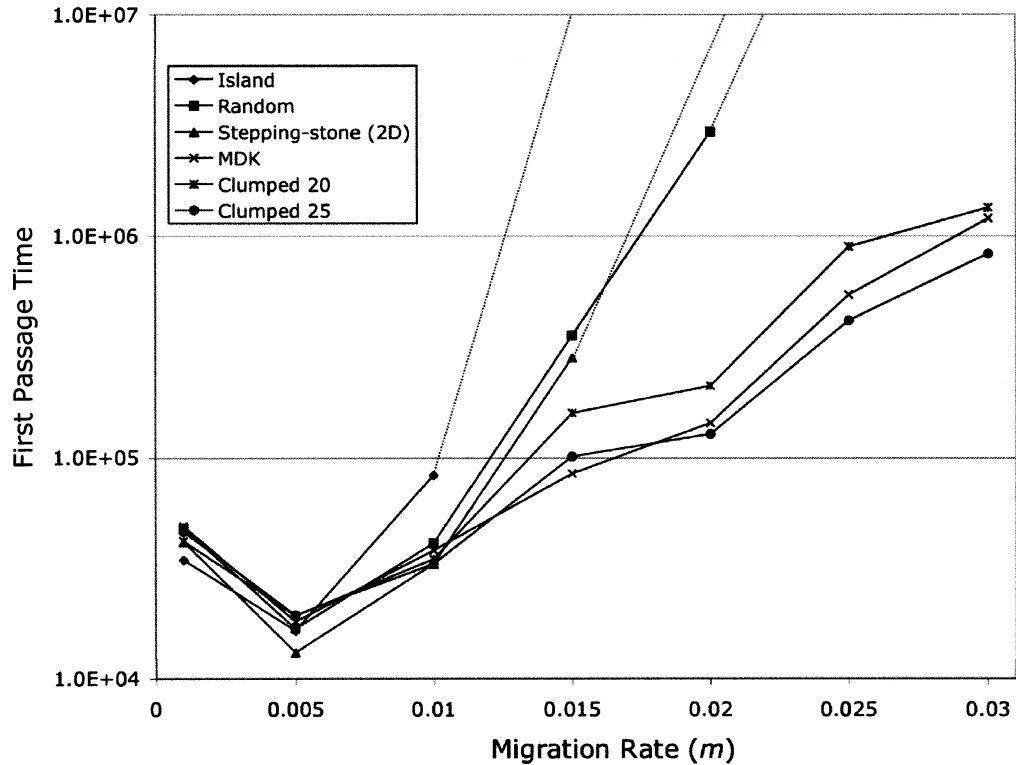


FIG. 3. The mean number of rounds taken for the simulation to progress from a state with all demes fixed for a to a state where all demes have  $p > 0.90$  (the first passage time), plotted as a function of the mean migration rate ( $m$ ). The dotted lines indicate a very large number of generations (greater than  $10^7$ , the maximum number of rounds in the simulation) for the island, random, and two-dimensional stepping-stone models.

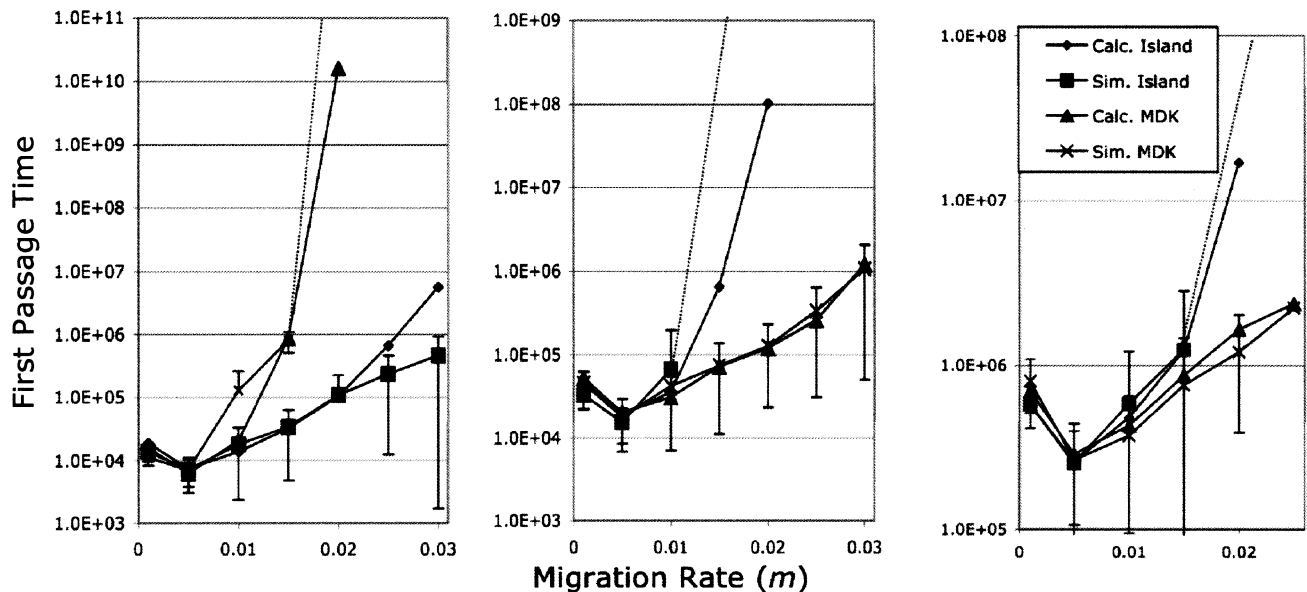


FIG. 4. Comparison of simulated and calculated first passage time for island and MDK models, for different numbers of demes: (a)  $D = 10$ ,  $N = 200$ , MDK(2,1); (b)  $D = 20$ ,  $N = 100$ , MDK(2,3); (c)  $D = 40$ ,  $N = 50$ , MDK(4,6). The dotted line indicates a large first passage time for the simulation runs, with a mean greater than the maximum number of generations allowed in the simulation ( $10^7$ ). As the number of individuals per deme decreases, the accuracy of the approximations improves.



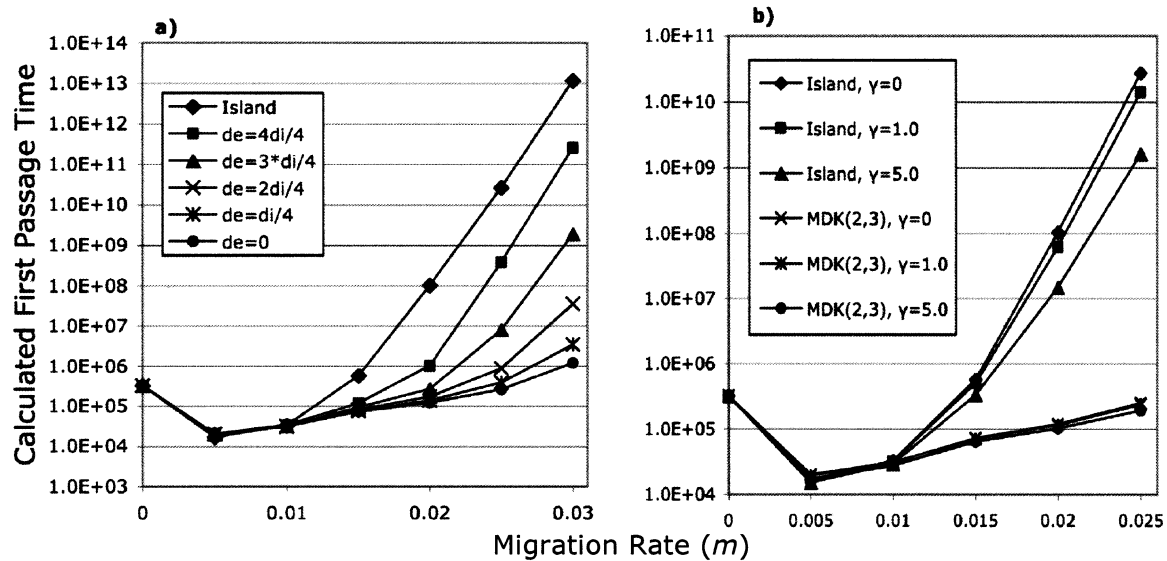


FIG. 5. Calculated first passage times (FPT) for models of differential export, for  $D = 20$ ,  $s = 0.05$ ,  $N = 100$ . (a) Decreasing export as a function of deme isolation, for different levels of the effect of isolation ( $d_e$ ). (b) Interdemic selection model, various population structures and levels of between-deme selection ( $\gamma$ ). Simulations match both mathematical models well (results not shown).

the fact that larger demes are less likely to be fixed for one allele or another for a given  $Ns$ .

#### Alternative Export Models

Figures 5a,b demonstrate the effects of decreased export of individuals due to isolation for a model with  $D = 20$ ,  $s = 0.05$ , and  $N = 100$ , as predicted by the Markov chain model. Results for the island model and uniform export MDK(2,3) model are shown for comparison. Increasing  $d_i$  from zero (the uniform export case) to  $d_e$  significantly increases the first passage time, though in all cases it remains an order of magnitude or more below the island case. In the interdemic selection model, it is apparent that increasing spatial complexity has a much greater effect on first passage times than does increasing  $\gamma$ , even when the new allele has a much greater effect on interdeme fitness than individual fitness.

#### The Effects of Increasing Isolation of Demes

In the simulations we examine only a few versions of the MDK model, MDK(4,6), MDK(2,3), and MDK(2,1) (for  $D = 40$ , 20, and 10, respectively). To further assess the effect of both the number of isolated demes, as well as the degree of isolation, we plot the calculated FPT relative to the island model, for a given number of isolated demes ( $k$ ), as a function of the degree of isolation of those demes ( $d/k$ ), for  $m = 0.005$ ,  $m = 0.015$ , and  $m = 0.025$  (Fig. 6), for  $Ns = 5$ ,  $D = 20$ , and  $N = 100$ . At  $m = 0.005$  increasing  $d$  and  $k$  increases the FPT, presumably because at lower migration rates in phases I and II are likely to occur in a clumped deme, and the new allele spreads more slowly to the isolated demes. In the most extreme case, FPT was increased from 25,000 generations to 41,000 generations. At higher migration rates, increasing  $d$  and  $k$  decreases the FPT. Even a small number of isolated demes (two of 20), with a modest degree of isolation (the

two demes receive half of the immigrants of other demes), reduced the FPT by over 80% relative to the island model in the  $m = 0.015$  case and by over three orders of magnitude in the  $m = 0.025$  case. The presence of a single isolated deme, if isolated by a great enough degree, can reduce the expected FPT by over 90%. However, because absolute FPT increases with migration rate in all models, at some point the difference between island and more complex models is moot—the process always takes so long that our assumptions of constant selection pressure, migration regime, and population size are no longer tenable.

#### DISCUSSION

Our results indicate that more complex forms of spatial structure, particularly those that increase the variance in interdeme connectivity, facilitate SB relative to island models. The introduction of even a modest number of isolated demes, one or two demes in a world of 20, may reduce the time taken for all demes to reach the more fit peak by an order of magnitude or more. The mechanism is straightforward. Isolated demes are more likely to wander across an adaptive valley because they receive fewer wild-type immigrants that tend to push demes back to the original peak. Once shifted to the more-fit peak, isolated demes are more difficult to unshift (again, because they receive fewer immigrants) and, hence, are more likely to induce a global peak shift.

The simulations and mathematics presented here relax some assumptions of earlier models. First, we examine more than two demes. Two-deme models, though presented as a representation of a single step in phase III, are inadequate for several reasons. Such models implicitly assume either a one-dimensional stepping-stone arrangement of demes or a global frequency of 50% for the more fit combination of alleles, both of which strongly bias results in favor of the SBT. Often, unidirectional migration is assumed, which fur-

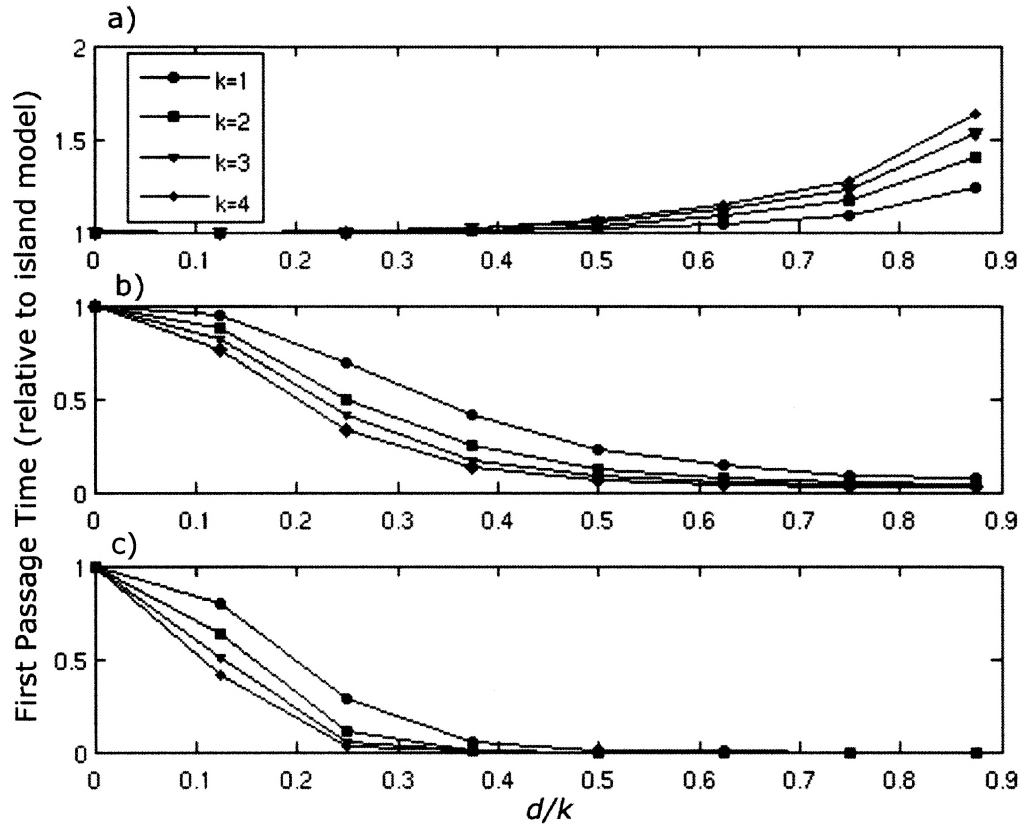


FIG. 6. (a) The decrease in calculated first passage time (FPT) relative to an island model ( $d = 0$ ), as the relative isolation of small numbers of demes increases, plotted for  $k = 1-4$ ,  $m = 0.005$ . (b) Same as above, but for  $m = 0.015$ ; (c)  $m = 0.025$ . Small numbers of isolated demes can substantially reduce the time taken to reach global fixation for the beneficial allele; this effect increases with increasing migration rate.

ther dissociates these models from reality (for further discussion see Gavrillets 1996). Second, our model assumes both stochastic migration between demes and stochastic change of gene frequencies within demes, factors Wright thought to be integral to the process. Third, we examine all three phases of the process together. In addition to being a more complete representation of the SBT, in our analysis the location of the deme that undergoes phases I and II has a significant effect on the probability of phase III proceeding. Also, the total number of generations taken to reach global fixation for the more fit peak is highly dependent on the amount of time spent waiting for phases I and II, and our results thus allow for more precise estimation of the actual time scale. Finally, we compare spatial arrangements of demes that incorporate variance in interpatch connectivity.

It is interesting to compare models of this sort with the two-deme stochastic model presented by Peck et al. (2000), which explicitly compared the likelihoods of phase III proceeding under alternative assumptions of deterministic and stochastic migration. In their model, migration was one-way from the deme fixed for AA. Phase III failed at low  $Nm$  because too few immigrants arrived to shift the less-fit deme in the time constraints of the model. Our results provide a different view of the process, where increasing migration decreases the likelihood of SB, because single demes that

drift to fixation are likely to be unshifted rapidly by immigration of *aa* individuals.

Our results build upon those of Barton and Rouhani (1991, 1993). Barton and Rouhani (1991) examine a two-dimensional stepping-stone model with the restriction  $s \ll m \ll sn^2$ , with  $n$  the number of demes along one dimension of the lattice. With the assumption of large  $m$ , they found deterministic stable equilibria at all and no demes shifted at every  $m$ , separated by an unstable manifold; they also found an optimal neighborhood size for the probability of fixation of a new underdominant allele. Barton and Rouhani (1993) examined an infinite island model and found equilibria similar to our Figure 2a, with deterministic progression to fixation at low  $m$  and two stable equilibria for higher  $m$ . Barton and Rouhani also obtained analytic approximations for the distribution of demic states, probabilities of spread of the new allele, and other interesting features, but they did not calculate passage times in the single-locus case or look at structures more complex than the island model.

Another insight may be gained by comparing spatial patterns with local interactions but little or no variance in deme connectivity (the two-dimensional stepping-stone and random models) to models with more variance. In our model, local interactions decrease the FPT relative to the island model, but increasing variance among deme connectivities further

decreases the FPT, in most cases substantially. One potential mechanism for this difference stems from the fact that most of the time spent waiting for fixation of the *A* allele is consumed by waiting for the first deme to shift, especially at high migration rates. Once one or two demes shift, phase III proceeds rapidly, often taking less than 10% of total FPT (results not shown). Demes that receive fewer wild-type immigrants are likely to shift more quickly than other demes, and because models with substantial variance necessarily include a few of these demes, these models spend less time waiting for phases I and II. Because our MDK model, which includes connectivity variance but no local interactions, performed as well or better than the clumped simulations, we conclude that variance is equally if not more important than local interactions. In this manner, our model is consistent with predictions made by Eldredge et al. (2005) regarding the importance of geographic structure in providing a mechanism for evolutionary stasis (though our model does not include spatially heterogeneous selection).

Our work is similar to that of Boorman and Levitt (1980), who examined the evolution of a social trait under frequency-dependent selection in metapopulations with complex structure (frequency-dependent selection is similar to our model of underdominance). Boorman and Levitt also concluded that spatial structure facilitates the spread of such a trait, given a migration rate that is neither too high (similar to our findings) or too low (a consequence of their deterministic analysis), and they also noted that the process is facilitated when the initially fixed deme is at an edge of the distribution of demes. However, they considered a different model of migration (equal import and export from every deme, though the number of demes connected to any given deme may vary). Though they briefly considered stochasticity as a possible cause for fixation in the initial deme, they envisioned subsequent spread as a purely deterministic process and modeled it as such. Our modeled allows us to avoid explicitly specifying an initially fixed deme and, thus, to explore the feasibility of the entire process.

Although our basic model includes uniform export from all demes regardless of isolation, we find that relaxing this assumption does not significantly alter our results, especially if individuals have some intrinsic tendency to migrate ( $d_e < d_i$ ). Even if distance has equivalent effects on both import and export ( $d_e = d_i$ ), first passage times are reduced by about two orders of magnitude from the island case for  $m > 0.015$ . We also find that interdemic selection of the kind envisioned by Wright, where demes with a higher mean fitness export more individuals, does not greatly affect first passage times. Complex spatial structure appears to have a substantially greater effect than does interdemic selection, even if the interdemic selection coefficient is substantially larger than the individual selection coefficient.

The degree to which these results bear upon a natural system depends on the relevant time scale. For relatively high migration rates ( $Nm = 1.5\text{--}3.0$ ), FPTs are hundreds of thousands or millions of generations. For long-lived species, these may translate into times so long that some assumptions fundamental to the SBT, such as relative constancy of the adaptive landscape or dispersal regime, may be unjustified.

Our model examines only a one-locus, two-allele genetic

system, and thus our results apply only to a simplified metaphor of the SBT. This choice was made to ease computations in the simulation and for comparison to other models that make the same assumption (Barton and Rouhani 1993; Gavrillets 1996; Peck et al. 1998, 2000), as well as models that examine underdominant chromosomal mutations (Lande 1985; Barton and Rouhani 1991). With multiple epistatic loci, fixations of single loci via drift in separate demes will likely revert to their original state quickly, unless they are combined immediately to produce a local peak shift. Put another way, the probability that the many correct alleles that constitute a more-fit adaptive peak will independently drift to fixation in the same deme seems vanishingly small. Our findings suggest that this may be less of an obstacle in metapopulations with complex spatial structure, because drift across adaptive valleys is favored in a small subset of the demes (the relatively isolated demes), which increases the likelihood that a single deme will drift to fixation for all necessary alleles.

Our results indicate that the theoretical plausibility of the SBT may have been underestimated by previous analyses that assumed a simple structure of migration and deterministic interactions among demes. If further work continues to support these findings, then research investigating more closely the structure of actual adaptive landscapes and transitions among them via the SBT may be justified. As more population-level genetic data become available, it may prove more feasible to look for the genetic signature of SB than to identify morphological characteristics. Our results suggest that the process is likely to begin in a relatively isolated subgroup that initiates a rapid selective sweep across the population. If the rate at which the allele spreads is high relative to the recombination rate, then many linked loci may be involved, a fact that could aid attempts to identify such sweeps (although it may obscure the loci responsible for initiating the shift). If variance in dispersal structure facilitates such shifts, we may expect populations of organisms with limited dispersal ability or particularly clumped habitat distributions to experience such sweeps more often than populations with a more homogeneous dispersal pattern. Although demonstrating that an adaptive valley was crossed remains a difficulty, comparing groups with differing dispersal patterns may provide some corroborative evidence for the SBT. Selective sweeps resulting from SB are likely to increase the number of substitutions in the population relative to background levels, thus repeated but infrequent episodes of this process may increase the variance in substitution rates over evolutionary time and could contribute to the overdispersion of the molecular clock (see Gillespie 1994).

It is not our goal to suggest that the shifting balance is responsible for a significant portion of adaptations found in nature. We agree with Coyne et al. (1997, 2000) when they asserted that the number of adaptations accounted for by Fisherian selection is many, whereas the number of adaptations accounted for by the SBT is currently none. However, a rigorous demonstration of operation of SB requires more effort than does a demonstration of Fisherian selection. Perhaps more importantly, we submit that the importance of a natural phenomenon is not determined by its frequency of occurrence alone. Importance may also be assigned to phenomena that differ from the norm and operate in a novel



fashion, as well as those that have lasting or significant consequences for the population in question. Because the SBT involves correlated changes in a large number of alleles, its operation may play an important role in the course of evolution taken by a population, even if the process itself occurs very infrequently or accounts for a small number of observed adaptations. In this manner, the SBT may be similar to Mayr's genetic revolutions (Mayr 1954), wherein small, isolated groups of individuals may effect large-scale genetic changes that would be unlikely in larger populations.

## ACKNOWLEDGMENTS

We thank K. Fitzgerald and J. Seger for helpful comments on the manuscript.

## LITERATURE CITED

- Adler, F. R. 2005. Modeling the dynamics of life. Thomson Brooks/Cole, Belmont, CA.
- Adler, F. R., and B. Nuernberger. 1994. Persistence in patchy irregular landscapes. *Theor. Popul. Biol.* 45(1):41–74.
- Barton, N. H., and S. Rouhani. 1991. The probability of fixation of a new karyotype in a continuous population. *Evolution* 45:499–517.
- . 1993. Adaptation and the “shifting balance.” *Genet. Res.* 61:57–74.
- Bhat, U. N., and G. Miller. 2002. Elements of applied stochastic processes. John Wiley and Sons, Hoboken, NJ.
- Blum, M. J. 2002. Rapid movement of a *Heliconius* hybrid zone: Evidence for phase III of Wright's shifting balance theory? *Evolution* 56:1992–1998.
- Boorman, S. A., and P. R. Levitt. 1980. The genetics of altruism. Academic Press, New York.
- Coyne, J. A., N. H. Barton, and M. Turelli. 1997. A critique of Sewall Wright's shifting balance theory of evolution. *Evolution* 51:643–671.
- . 2000. Is Wright's shifting balance theory important in evolution? *Evolution* 54:306–317.
- Crow, J. F., W. R. Engels, and C. Denniston. 1990. Phase three of Wright's shifting-balance theory. *Evolution* 44:233–247.
- Eldredge, N., J. N. Thompson, P. M. Brakefield, S. Gavrillets, D. Jablonski, J. B. C. Jackson, R. E. Lenski, B. S. Lieberman, M. A. McPeck, and W. Miller. 2005. Dynamics of evolutionary stasis. *Paleobiology* 31:133–145.
- Ewens, W. J. 1979. Mathematical population genetics. Springer-Verlag, New York.
- Fisher, R. A. 1930. The genetical theory of natural selection. Oxford Univ. Press, Oxford, U.K.
- Gavrillets, S. 1996. On phase three of the shifting balance theory. *Evolution* 50:1034–1041.
- Gillespie, J. H. 1994. Substitution models in molecular evolution. II. Exchangeable models from population genetics. *Evolution* 48:1101–1113.
- Hanski, I. 1994. A practical model of metapopulation dynamics. *J. Anim. Ecol.* 63:151–162.
- Lande, R. 1979. Effective deme sizes during long-term evolution estimated from rates of chromosomal rearrangement. *Evolution* 33:234–251.
- . 1985. The fixation of chromosomal rearrangements in a subdivided population with local extinction and colonization. *Heredity* 54:323–332.
- Mayr, E. 1954. Change of genetic environment and evolution. Pp. 157–180 in J. Huxley, ed. *Evolution as a process*. Allen and Unwin, London.
- Peck, S. L., S. P. Ellner, and F. Gould. 1998. A spatially explicit stochastic model demonstrates the feasibility of Wright's shifting balance theory. *Evolution* 52:1834–1839.
- . 2000. Varying migration and deme size and the feasibility of the shifting balance theory. *Evolution* 54:324–327.
- Phillips, P. C. 1993. Peak shifts and polymorphism during phase three of Wright's shifting-balance process. *Evolution* 47:1733–1743.
- Provine, W. 1971. The origins of theoretical population genetics. Univ. of Chicago Press, Chicago.
- Wade, M., and C. Goodnight. 1991. Wright's shifting balance theory: an experimental study. *Science* 253:1015–1018.
- . 1998. The theories of Fisher and Wright in the context of metapopulations: when nature does many small experiments. *Evolution* 52:1537–1553.
- . 2000. The ongoing synthesis: a reply to Coyne, Barton, and Turelli. *Evolution* 54:317–324.
- Wright, S. 1931. Evolution in Mendelian populations. *Genetics* 16:97–159.

Corresponding Editor: S. Gavrillets